http://dx.doi.org/10.5012/bkcs.2013.34.6.1755

Electrodeposition of Graphene–Zn/Al Layered Double Hydroxide (LDH) Composite for Selective Determination of Hydroquinone

Yeonji Kwon and Hun-Gi Hong*

*Department of Chemistry Education, Seoul National University, Seoul 151-748, Korea. *E-mail: hghong@snu.ac.kr*
Received December 31, 2012, Accepted March 19, 2013

A graphene-Zn/Al layered double hydroxide composite film was simultaneously prepared by electrochemical deposition on the surface of a glassy carbon electrode (G-LDH/GCE) from the mixture solution containing GO and nitrate salts of Zn^{2+} and Al^{3+}. The modified electrode showed good electrochemical performances toward the simultaneous electrochemical detection of hydroquinone (HQ), catechol (CA) and resorcinol (RE) due to the unique properties of graphene (G) and LDH such as large active surface area, facile electronic transport and high electrocatalytic activity. The redox characteristics of G-LDH/GCE were investigated with cyclic voltammetry and differential pulse voltammetry. The well-separated oxidation peak potentials, corresponding to the oxidation of HQ, CA and RE, were observed at 0.126 V, 0.228 V and 0.620 V respectively. The amperometric response of the modified electrode exhibited that HQ can be detected without interference of CA and RE. Under the optimized conditions, the oxidation peak current of HQ is linear with the concentration of HQ from 6.0 μM to 325.0 μM with the detection limit of 0.077 μM (S/N=3). The modified electrode was successfully applied to the direct determination of HQ in a local tap water, showing reliable recovery data.

Key Words : Graphene, Layered double hydroxide, Hydroquinone, Simultaneous detection, Differential pulse voltammetry

Introduction

Hydroquinone (HQ), known as 1,4-dihydroxybenzene, is a phenolic compound which is widely used in depigmenting agents, medicines, cosmetic products, antioxidant and photography chemicals.[1] Because it is hazardous to human health and has low levels of degradability in the environment, it is considered as an environmental pollutants to be monitored in aquatic environment by the US environmental Protection Agency (EPA) and the European Union (EU).[2] Therefore, it is necessary to develop highly selective and sensitive analytical methods for the detection of hydroquinone. So far several analytical methods such as capillary electrochromatography,[2] chromatography,[3] and spectrophotometry[4] have been developed to analyze HQ. However, most of these methods have some disadvantages such as complicated pretreatment, time-consuming, low sensitivity and high cost. Electrochemical methods provide not only an easy and rapid way in environmental analysis but also simple operation, low cost, cheap instrument, high sensitivity, excellent selectivity, and fast response. In environmental samples, HQ often coexists with its isomers such as catechol (1,2-dihydroxybenzene, CA) and resorcinol (1,3-dihydroxybenzene, RE), and the three isomers of dihydroxybenzene have similar structures and properties. Therefore, it is important to detect HQ without any interference from CA and RE. When using electrochemical methods, more attentions are focused on the simultaneous determination of HQ and CA because their redox peaks are overlapped at ordinary electrodes. For example, Qi and Zhang reported that a simple and high selective electrochemical method for simultaneous determination of HQ and CA has been developed at a glassy carbon electrode modified with multiwall carbon nanotubes (MWCNT).[5] Other chemical modification methods using GCE for simultaneous determination of HQ and CA were reported by Wang[6] *et al.* with penicillamine, Zhao[7] *et al.* with a composite of MWCNT and negatively charged polyamidosulfonic acid, and Yin[8] *et al.* with graphene-chitosan composite film.

Layered double hydroxides (LDHs), known as hydrotalcite-like multifunctional materials or anionic clays, are generally represented by the formula $[M^{II}_{1-x}M^{III}_{x}(OH)_2]^{x+}(A^{n-})_{x/n}\cdot mH_2O$, where M^{2+} and M^{3+} are divalent and trivalent metal cations, respectively, and anion (A^{n-}) located in the gallery between the layers.[9] The layered structures have received many attentions because of their attractive properties such as large surface area, tunable composition, exchangeable anions, thermal stability, chemical inertia, well-defined layered structure and low cost.[10] Using these properties, LDHs have been widely investigated for a wide range of areas such as catalysis, biocatalysis, sensors, drug delivery and adsorbents.[11-13] Recently, many reports have demonstrated the successful utilization of LDH as an electrode modification material.[14,15] Despite its usefulness, the weak conductivity of LDH sometimes results in poor charge transport restricting its electrochemical performance. However, the incorporation of conducting materials into LDHs has shown improved electrical properties. For example, all the composite films of carbon nanotube/Zn/Al-LDH,[16] graphene/Ni/Al-LDH,[17] graphene/Co/Al-LDH,[18] activated carbon/Co/Al-LDH,[19] and gold nanoparticle/Mg/Al-LDH[20] show improved electrochemical activities on HQ detection,[16] supercapacitor materials[17-19] and methanol oxidation.[20]

Graphene(G), a monolayer of carbon atoms in a closely packed honeycomb two-dimensional lattice, has attracted considerable attentions due to its unique structure, electronic transport property, chemical property, large surface area and excellent electrocatalytic characteristics compared to other carbon-based materials.[21-23] For these reasons, graphene has been applied to a wide range of electrical fields such as nanocomposites, chemical and biosensors, batteries, supercapacitors, and nanoelectronics.[24-27] Graphene oxide (GO), known as a precursor for graphene synthesis by either thermal or chemical reduction process,[28] has a two-dimensional plane and good electrical characteristics. Furthermore, GO is more hydrophilic than graphene and can be easily dispersed in an aqueous solution because it contains oxygen functional groups (*e.g.* -OH, C-O-C, -COOH, etc). Recently, GO in a solution can be electrochemically reduced directly to yield graphene on an electrode surface using electrochemical methods.[29,30]

In this work, we demonstrate a new procedure using graphene to improve the electrocatalytic function of LDH as a support material for simultaneous determination of HQ, CA and RE. The composite film, consisting of graphene and LDH, presented the advantages such as large surface area, unique electrochemical properties and strong electrocatalytic activity due to synergic and native characteristics of the two components. The composite film is simultaneously formed on the surface of GCE by electrodeposition from the mixture solution containing colloidal GO and nitrate salts of Zn^{2+} and Al^{3+} as components forming LDH in one pot. This direct one-pot synthesis has advantage that soluble GO is not agglomerated to graphene nanosheets by reduction during electrodeposition because of the electric repulsion between negatively charged GO and positively charged host layer of LDH formed in the electrodeposition. In addition, this synthesis is simple, facile, fast and inexpensive for the fabrication of the modified electrode compared to other previous reports[17,18] using immobilization and hydrothermal methods. The proposed method exhibited good analytical performances in the simultaneous determination of HQ, CA and RE and has been applied to determination of HQ in a local tap water sample with high sensitivity and fast response.

Experimental

Apparatus and Reagents. The Electrochemical measurements were carried out with a conventional three-electrode system (CHI 842B and 760B C.H. Instruments, Inc., U.S.A). A bare or modified glassy carbon electrode (GCE) was used as a working electrode while Ag/AgCl/ KCl (3.0 M), and Pt wire were used as the reference and counter electrodes, respectively. All measurements were carried out at room temperature. Images of the modified electrode surface were obtained using a field emission scanning electron microscopy (FE-SEM, Hitachi S-4800). Electrochemical impedance spectroscopy (EIS) measurements were performed in the presence of 5 mM $K_3[Fe(CN)_6]$ as a redox probe and 0.1 M KCl in the frequency range from 0.01 to 100,000 Hz. The amplitude of the applied sine wave potential was 5 mV with the formal potential set at 0.25 V. The differential pulse voltammograms were obtained by scanning the potential from −0.2 to 0.8 V with the following pulse amplitude, 0.05 V; pulse width, 0.05s; sample width, 0.0167s; pulse period, 0.2s.

Graphite powder (400 mesh), $Zn(NO_3)_2{\cdot}6H_2O$, $Al(NO_3)_3{\cdot}9H_2O$, CA, HQ and RE were purchased from Sigma-Aldrich (USA). All other reagents were of analytical grade and were used as received without further purification. Phosphate buffer solution (PBS, 0.1 M) was prepared by mixing a stock solution of 0.1 M NaH_2PO_4, and 0.1 M Na_2HPO_4, and the pH was adjusted by NaOH or HCl. All solutions were prepared with deionized water obtained from an ultrapure water purification system (LabTech, Korea) with a resistivity of not less than 18.2 MΩ cm.

Preparation of Graphene Oxide. Graphene oxide (GO) was prepared using a modified Hummers method.[31] In brief, graphite powder was oxidized by a hot solution (80 °C) of concentrated H_2SO_4 containing $K_2S_2O_8$ and P_2O_4. The pre-oxidized GO was placed in concentrated H_2SO_4 at 0 °C. $KMnO_4$ was gradually added while stirring and cooling the mixture, so that the temperature of the mixture remained below 20 °C. The obtained GO was washed with 10% HCl and deionized water until it was neutral. The GO was then centrifuged to remove the aggregated GO.

Preparation of Graphene-Layered Double Hydroxide on Glassy Carbon Electrode. Prior to the modification, the GCEs (3 mm in diameter) were polished with 0.3 and 0.05 μm alumina powder/water slurry on a polishing pad. The GCE was then rinsed, after which it was sonicated in deionized water and ethanol for each 5 minute. The graphene-layered double hydroxide composite modified GCE (G-LDH/GCE) was constructed by slight modifying reported methods previously.[14,32] The polished and cleaned GCEs were immersed in 0.1 M $HClO_4$ and then were carried out using a potential cycling between −0.2 and 1.8 V at a scan rate of 50 mV/s for 10 minutes. After rinsing the electrode with deionized water, it was dried at room temperature. The G-LDH composite film was electrodeposited onto the electrode surface by cathodic reduction using a solution containing 12.5 mM $Zn(NO_3)_2{\cdot}6H_2O$ as the Zn^{2+} source, 7.5 mM $Al(NO_3)_3{\cdot}9H_2O$ as the Al^{3+} source, 1.2 M KNO_3 as the supporting electrolyte and GO aqueous solution (1 mg/mL). Cathodic deposition was performed by applying potential of −1.65 V for 120s under stirring. After the electrodeposition process, the modified electrode was rinsed with deionized water to remove physically adsorbed material. For comparison with the G-LDH/GCE, the LDH/GCE and G/GCE were also fabricated under the same experimental conditions. The LDH/GCE was electrodeposited using a solution containing 12.5 mM $Zn(NO_3)_2{\cdot}6H_2O$, 7.5 mM $Al(NO_3)_3{\cdot}9H_2O$, and 1.2 M KNO_3. The G/GCE was electrodeposited using a solution containing a GO aqueous solution (1 mg/mL) and 1.2 M KNO_3 as the supporting electrolyte.

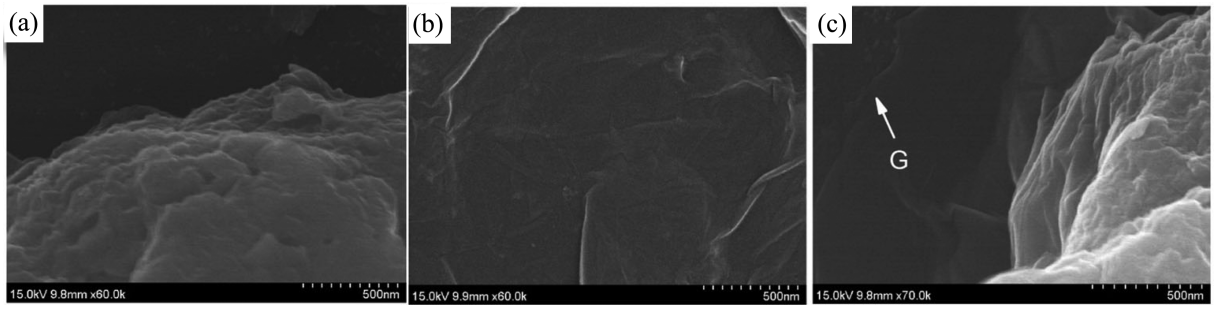

Figure 1. SEM images of LDH (a), reduced graphene oxide (b) and G-LDH (c) films on GCE.

Results and Discussion

The Characterization of G-LDH Films. The morphologies of the electrodeposited materials on GCE are shown in Figure 1. Figure 1(a) typically shows that the electrodeposited LDH films have a layered structure on the surface of glassy carbon electrode. The presence of well-defined layered structure can increase the effective surface area and accumulate more analytes in the gallery between the layers and on the electrode surface. Figure 1(b) shows a SEM image of reduced GO electrodeposited from a solution containing GO and 1.2 M KNO_3 as the supporting electrolyte. We can observe that the electrodeposited graphene consists of transparent and wrinkled silk-like surface, which is associated with the presence of ultrathin graphene nanosheets. These unique features of graphene films are highly beneficial in maintaining a high surface area on the electrode. The G-LDH composite is shown in Figure 1(c). It can be seen that the G-LDH composite film comprises not only a layered structure coming from traditional hydrotalcite anionic clays but also a wrinkled silk-like two-dimensional graphene nanosheet structure. This result indicates that the G-LDH composite can be fabricated by electrodeposition with the mixture electrolytes solution containing GO colloidal particles, di- and trivalent metal cations consisting of the LDH structure itself.

Electrochemical impedance spectroscopy measurements can be used to evaluate the effect of LDH, G and G-LDH films on the kinetics of a redox reaction at the modified GCE electrodes. Figure 2 presents the complex impedance plots for a bare and various modified GCEs at a potential of 0.25 V in the presence of 5 mM $Fe(CN)_6^{3-}$. The Nyquist plots for the electrodes is characterized by a semicircle at high frequency and a linear Warburg line at an angle of 45° in the low frequency region. The semicircle corresponds to a parallel combination of the charge transfer resistance with the double layer capacitance, while the linear response is related to mass transfer effects. The impedance plots for GCEs modified by the electrodeposition differ significantly from that of the bare electrode. As shown in Figure 2, all the electrodes show the linear line at an angle of 45° in the low frequency region. However, the diameter of the semicircle is largely different each other. For example, the semicircle of LDH/GCE (8.8 kΩ) increased as compared to that of the bare GCE (5.5 kΩ). This result suggests that the LDH acts as an insulating material due to its weak electrochemical characteristics. The semicircle of G/GCE (2.1 kΩ) decreases dramatically due to the fast electron transfer and excellent electrocatalytic characteristics of graphene oxide. When LDH is co-electrodeposited with G, the semicircle slightly increases compared to that of the G/GCE, indicating that the charge transfer resistance of the G-LDH/GCE (2.7 kΩ) is larger than that of the G/GCE. These impedance results show that the exfoliated G nanosheets could improve the electrochemical properties of GCE modified with LDH only when G is combined with LDH.

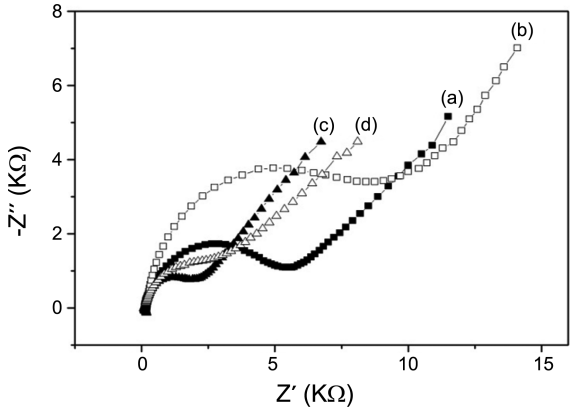

Figure 2. Nyquist plots of the electrochemical impedance spectroscopy (EIS) for bare GCE (a), LDH/GCE (b), G/GCE (c) and G-LDH/GCE (d) in 5 mM $Fe(CN)_6^{3-}$ at a potential of 0.25 V.

Cyclic Voltammetric Responses of the Modified GCEs to HQ. Figure 3 shows cyclic voltammograms of HQ at bare GCE (a), LDH/GCE (b), G/GCE (c), and G-LDH/GCE (d) in 0.1 M PBS (pH 6.5). At the bare GCE, the anodic and cathodic peak potentials of HQ were at 0.34 and −0.05 V, respectively. The peak potential separation (ΔEp) was *ca.* 0.39 V. This large ΔEp indicates that the electrochemical redox process of HQ exhibits kinetically quite slow electron transfer characteristics at the bare GCE. On the other hand, at the LDH/GCE (b), the oxidation peak potential negatively shifts to 0.125 V, and the reduction peak potential positively shifts to 0.080 V with a peak separation (ΔEp) value of 0.045 V. This large shift in the peak potential and large decrease in the ΔEp indicate that the reversibility of HQ is greatly improved by electrochemical catalytic activity of

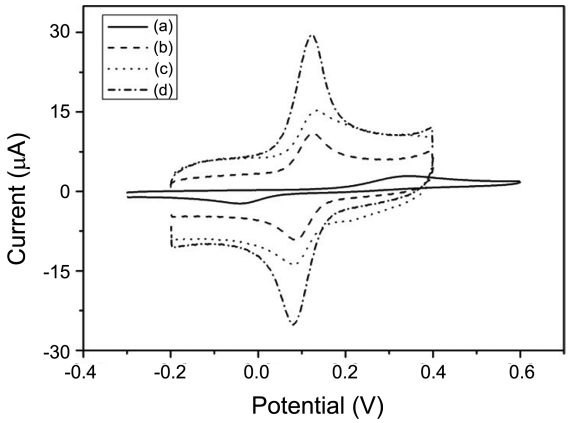

Figure 3. Cyclic voltammograms of 0.1 mM HQ in 0.1 M PBS (pH=6.5) at bare GCE (a), LDH/GCE (b), G/GCE (c) and G-LDH/GCE (d). Scan rate: 100 mV/s.

LDH films on GCE. This can be attributed to the structural features of layered double hydroxide and chemical inertia of LDH films. These results show that the presence of LDH on the GCE surface can lead to the accumulation of more HQ molecules into the gallery between the positively charged lamellar structures, resulting in the large surface area on the electrode surface. Hence, the effective surface of the electrode is increased. However, dramatically enhanced electrochemical signal of HQ cannot be observed at the LDH/GCE. Similarly, at the G/GCE (c), the anodic and cathodic peak potentials of HQ appeared at 0.134 and 0.080 V, respectively, and the ΔEp value for HQ was 0.054 V. These electrochemical traits demonstrate that the electrochemical reversibility of HQ is substantially improved due to the unique properties of graphene, which accelerates the electron transfer and increases active surface area of the electrode. However, there is no peak current enhancement which is favorable to detection of HQ. As shown in Figure 3(d), at the G-LDH/GCE, the anodic and cathodic peak potentials of HQ appeared at 0.124 and 0.080 V, respectively, and the ΔEp value for HQ was 0.051 V. These electrochemical characteristics seem to be quite similar to those data observed at both the LDH/GCE and G/GCE. However, remarkable increases of the anodic and cathodic peak currents were observed. The redox peak currents of HQ observed at the G-LDH/GCE were 11.02, 3.01 and 2.6 fold higher than those at the bare GCE, LDH/GCE and G/GCE, respectively. These facts indicate that the incorporation of G into the LDH matrix can efficiently promote the weak conductivity due to poor charge transport of LDH. Besides, G-LDH composite have a larger electroactive surface area than those of the individual components, demonstrating that combining the advantageous characteristics of G and LDH can exhibit excellent electrical conductivity and catalytic activity toward the redox reaction of HQ. Furthermore, the ratio of the anodic (I_{pa}) and cathodic (I_{pc}) peak current (I_{pa}/I_{pc}) is close to 1, which is a typical characteristics of a quasi-reversible process.

Effect of Scan Rate (ν). The effect of scan rate on the voltammetric response of the G-LDH/GCE in 0.1 M PBS

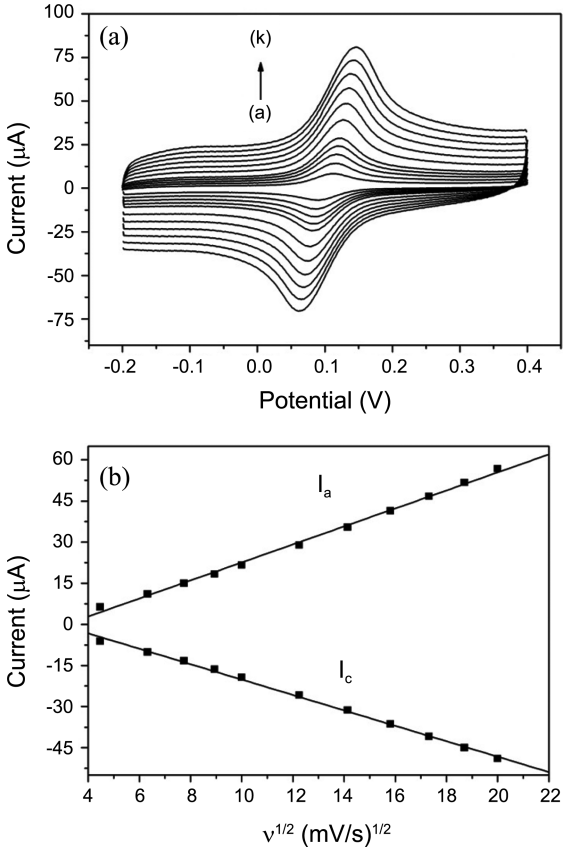

Figure 4. Cyclic voltammograms of 0.1 mM HQ in 0.1 M PBS (pH=6.5) at G-LDH/GCE at different scan rates; (a)-(k) 20, 40, 60, 80, 100, 150, 200, 250, 300, 350 and 400 mV/s (a). Plots of anodic and cathodic peak currents *vs*. square root of scan rate (b).

containing 0.1 mM HQ was investigated. As shown in Figure 4(a), both the anodic and cathodic peak currents of HQ increased with an increase in the scan rate from 20 to 400 mV/s. The redox peak currents show a good linear relationship with the square root of the scan rate (Figure 4(b)). The regression equations were $i_{pa}(uA) = 3.28\ \nu^{1/2} - 10.2$ and $i_{pc}(uA) = 7.98 - 2.82\ \nu^{1/2}$ with the same correlation coefficient R of 0.997, respectively. These results strongly suggest that the HQ oxidation and reduction are under diffusion control process at the modified electrode.

Effect of Buffer pH. In order to optimize the buffer pH condition of detecting HQ at the G-LDH/GCE, as shown in Figure 5(a), the redox peak potential and peak current of hydroquinone were investigated over a pH range of 5.5-8.0 in phosphate buffer solution. Figure 5(b) presents that the redox peak currents increased until the pH value reached 6.5 and then decreased. The maximum peak current was obtained at pH of 6.5. Thus, we have chosen 6.5 as the optimum pH value for the electrochemical detection of HQ. When the pH value is higher than 8.0, the peak current rapidly decreases. This could be due to the shortage of proton participating in the electrochemical reaction of hydroquinone. At the higher pH solution, hydroquinone molecule is deprotonated to its mono- and dianion form, which might bring in electrostatic repulsion from G-LDH composite film. This could make the

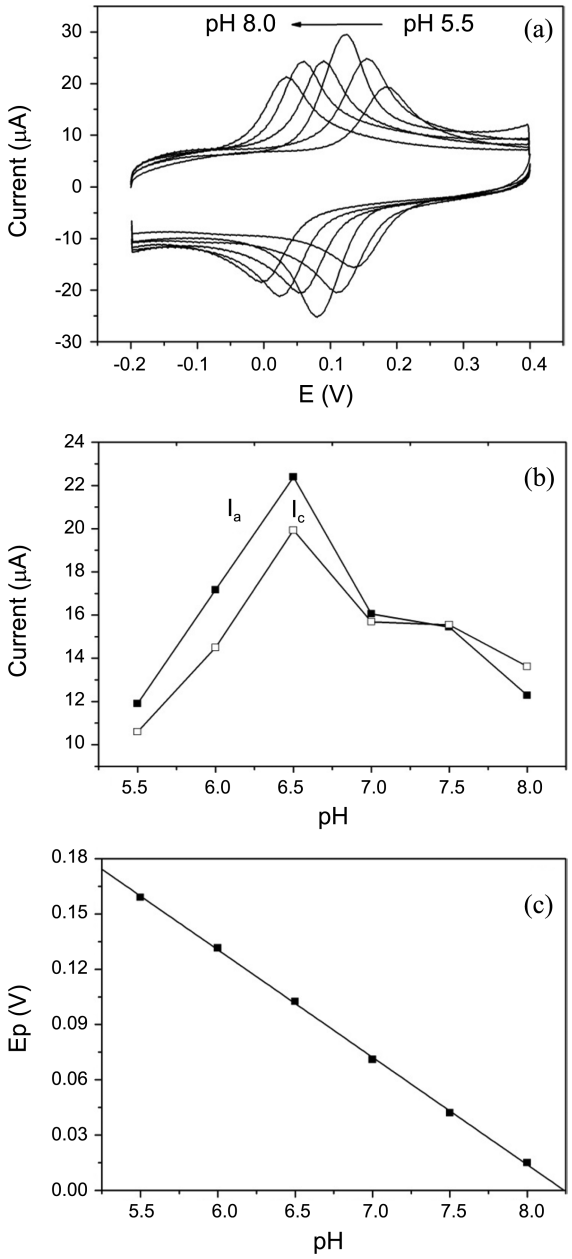

Figure 5. The effect of pH on the Cyclic voltammograms (a), peak current response (b) and the redox peak potential (c) of 0.1 mM HQ in 0.1 M PBS (pH=6.5) at G-LDH/GCE with scan rate 100 mV/s.

redox reaction of hydroquinone more difficult resulting in low peak current. As shown in Figure 5(c), the redox peak potential, $E_p = (E_{pa}+E_{pc})/2$, of HQ shifts to more negative values with an increase in the pH values. The linear regression equations are $E_p(V) = 0.480\text{-}0.058$ pH (R=0.999) for HQ. The slopes of E_p *vs*. pH are close to the theoretical value of 58.5mV/pH, indicating that a two electrons and two protons process occurs at G-LDH/GCE. All these electrochemical features of HQ observed in Figure 5 were also obtained quite similarly for the electrochemical reaction of CA and RE as dihydroxybenzene isomers (data not shown) in the same experimental condition as in Figure 5.

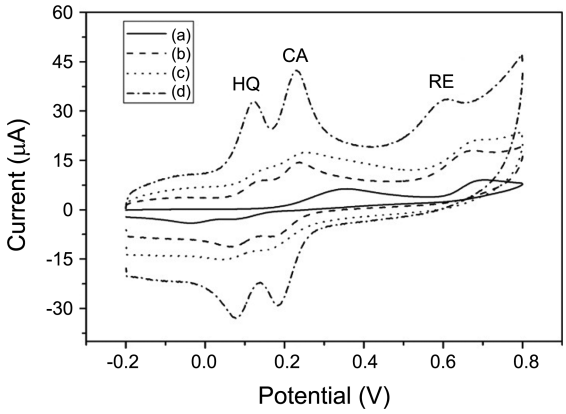

Figure 6. Cyclic voltammograms of HQ, CA and RE (0.1 mM of each) in 0.1 M PBS (pH=6.5) at bare GCE (a), LDH/GCE (b), G/GCE (c) and G-LDH/GCE (d). Scan rate: 100 mV/s.

Simultaneous Determination of HQ, CA and RE. CA and RE are the isomers of HQ and usually coexist in test samples. Therefore, it is important to remove the interference of the isomers for the selective determination of HQ. At first, the electrochemical determination of HQ, CA and RE in the mixture was investigated using cyclic voltammetry. Cyclic voltammograms of an equimolar (0.10 mM) concentration mixture of HQ, CA and RE in 0.1 M PBS (pH = 6.5) are shown in Figure 6. An overlapped wide oxidation peak at about 0.36 V is observed at the bare GCE (a), indicating that the bare GCE cannot separate oxidation peaks of HQ and CA. Although the redox peak of HQ can be barely separated from that of CA at the LDH/GCE (b) and G/GCE (c), their peak currents are not large enough to be separated from the mixture solution. This trend could be worse in the low micromolar concentration mixture of dihydroxybenzene isomers. In contrast, at G-LDH/GCE (d), the anodic and cathodic peak of HQ and CA are well developed and their peak currents are much higher than those at the LDH/GCE and G/GCE. For HQ, the I_{pa} is 4.2 and 3.7 times higher than those at LDH/GCE and G/GCE, respectively. At the same time, three well-separated oxidation peak potentials were observed at 0.126 V, 0.228 V and 0.620 V corresponding to the oxidation of HQ, CA and RE, respectively. The anodic (ΔE_{pa}) and cathodic (ΔE_{pc}) peak potential differences between HQ and CA are up to 105 mV and 104 mV, respectively, which suggest that the simultaneous determination of HQ, CA and RE are considerably more sensitive compared with those at LDH/GCE and G/GCE. For the simultaneous and quantitative determination of HQ and CA at the G-LDH/GCE, differential pulse voltammetry was used because of its higher current sensitivity and better resolution. The individual determination of HQ or CA in their mixtures was investigated when the concentration of one species changed, whereas others remained constant. Figure 7(a) showed the differential pulse voltammogram of HQ with its different concentrations in 0.1 M phosphate buffer solution (pH 6.5) containing 25.0 μM CA and 50.0 μM RE. The anodic peak current of HQ is proportional to its concentration from 3.0 μM to 100.0 μM,

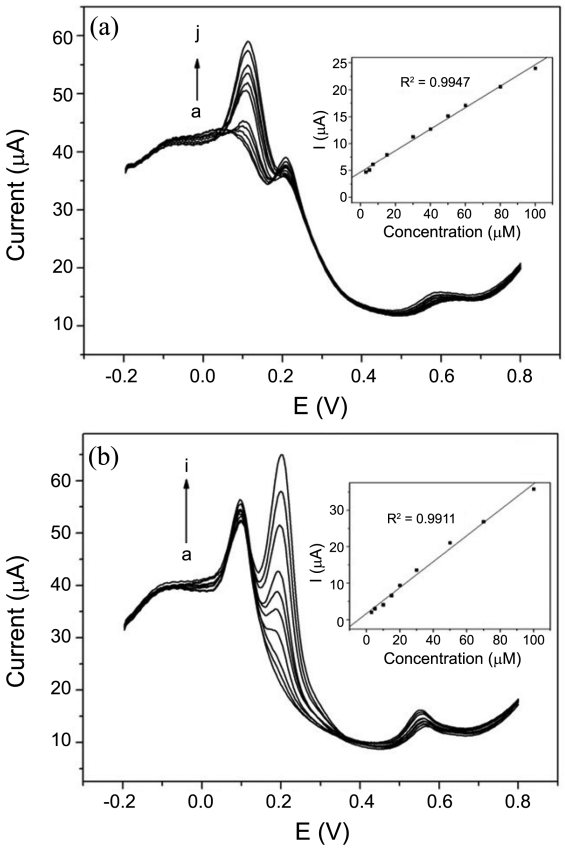

Figure 7. Differential pulse voltammograms of HQ at G-LDH/GCE in the presence of 25 μM CA and 50 μM RE in 0.1 M PBS (pH=6.5). HQ concentrations (from a to j): 3, 5, 7, 15, 30, 40, 50, 60, 80 and 100 μM (a), Differential pulse voltammograms of CA at G-LDH/GCE in the presence of 25 μM HQ and 50 μM RE in 0.1 M PBS (pH=6.5). CA concentrations (from a to i): 3, 5, 10, 15, 20, 30, 50, 70 and 100 μM (b).

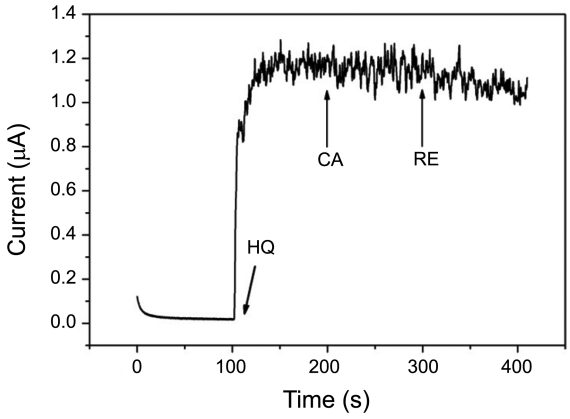

Figure 8. Amperometric response of the G-LDH/GCE to the sequential addition of 25 μM HQ, 25 μM CA and 25 μM RE under stirring 0.1 M PBS (pH=6.5). The applied potential at the modified working electrode was 0.125 V.

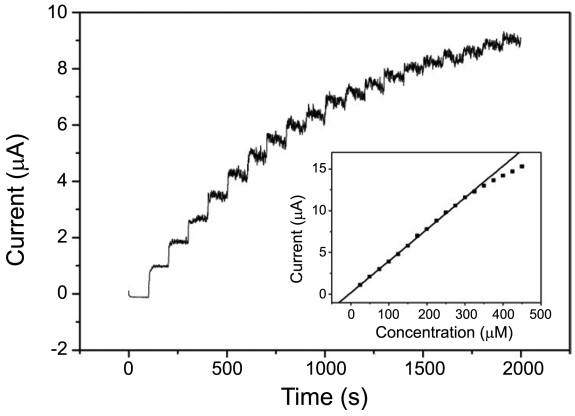

Figure 9. Amperometric response of the G-LDH/GCE to successive injection of 25 μM HQ in 0.1 M PBS (pH=6.5) under stirring. Applied potential: 0.125 V. Insert: the calibration curve of the amperometric current vs. concentration of HQ.

as shown in the inset of Figure 7(a). Similarly, the oxidation peak current of CA linearly increases with its concentration from 3.0 μM to 100.0 μM when keeping the concentration of HQ and RE constant at 25.0 μM and 50.0 μM as shown in Figure 7(b). Therefore, the G-LDH/GCE provides sensitive, selective, and quantitative determination of HQ and CA without interference for each other.

Amperometric Responses of the G-LDH/GCE. We also investigated the amperometric response of the G-LDH/GCE to the oxidation of HQ. From Figure 8, it can be seen that an increase of the oxidation current was obtained with the addition of 25 μM HQ under stirring electrolyte solution at the applied potential of 0.125 V. Afterward the injection of identical concentrations of CA and RE, there were only negligible current responses generated by CA and RE when compared with the dramatic current increase due to the addition of HQ. This behavior shows that the existence of CA and RE are not interfering in the selective determination of HQ at the G-LDH/GCE. Figure 9 displays a typical amperometric response of the G-LDH/GCE upon the successive addition of HQ in the 0.1 M PBS (pH 6.5) aqueous solution under stirring at 0.125 V. A remarkable increase of the oxidation current was observed upon a subsequent addition of HQ. Inset is the calibration curve of the oxidation peak current *vs*. the concentration of HQ. A linear response was observed in the range from 6 μM to 325 μM with a correlation coefficient of 0.991, and the regression equation was $i_{pa}(\mu A) = 0.169+0.038$ μM. The detection limit is 0.077 μM with a signal-to-noise ratio of 3, and the time to reach the 98% steady state response is less than 3s. The electroanalytical characteristics of some electrodes using other modification strategies to detect HQ are summarized in Table 1. The sensitivity and detection limit of our new strategy improve those of the other reported modified electrodes.

Stability and Reproducibility of the G-LDH/GCE. The stability of the G-LDH/GCE was investigated by measuring the current response with a 0.1 mM HQ. After 100 continuous potential scanning cycles, the anodic and cathodic peak currents remain more than 98% of the initial current response, respectively. In addition, there was no observed peak potential shift in the cyclic voltammograms of HQ, indicating that the G-LDH composite on the surface of GCE is

Table 1. Comparison of analytical performance of on different modified electrodes

Electrode	Method	Linear range (μM)	Limit of Detection	Reference
LDHf/GCE	DPV	12-800	9	14
Graphene/GCE	DPV	1-50	0.015	33
Graphene-chitosan/GCE	DPV	1-300	0.75	8
MWCNT/GCE	DPV	1-100	0.75	5
Penicillamine/GCE	DPV	15-115	1	6
PASA/MWCNT/GCE	DPV	6-400	1	7
Mesoporous carbon modified/GCE	Amperometry	10-200	0.076	34
Pt-graphene modified/GCE	DPV	20-145	6	35
MWNTs/multielectrode array	Amperometry	1-100	0.3	36
Activated/GCE	DPV	0.5-200	0.16	37
Mesoporous platinum electrode	DPV	20-1000	-	38
G-LDH/GCE	Amperometry	6-325	0.077	This work

LDHf: Zn/Al layered double hydroxide film; MWCNT: multiwall carbon nanotubes; PASA: poly-amidosulfonic acid.

Table 2. Determination of HQ in local tap water samples

Sample No.	added HQ (μM)	found HQ (μM)	RSD (%)	Recovery (%)
1	30	29.38	4.71	97.9
2	15	15.50	4.21	103.3
3	10	9.8	3.5	98.14

stable. To compare the reproducibility further, five different GCEs were modified with G-LDH composite film. And these electrodes were kept at room temperature for a week after their first measurements with a 0.1 mM HQ. A week later, those electrodes were measured again and the peak currents of them remained more than 97% and the relative standard deviation (R.S.D) was calculated 1.1%, which indicated that the G-LDH composite on the surface of GCE shows an acceptable level of reproducibility.

Sample Analysis Using G-LDH/GCE. In order to ascertain applicability of the newly devised electrode for the selective determination of HQ, local tap water samples were tested for quantitative analysis. The spike and recovery experiments were performed by measuring the differential pulse voltammetry responses to the samples containing the known concentrations of HQ because the amount of HQ was unknown in local tap water samples. The analytical performance of the G-LDH/GCE from the sample recovery tests are summarized in Table 2, showing that the recovery of HQ were in the range from 97.9% to 103.3%. These results demonstrate that the G-LDH/GCE could be exploited for the determination of HQ content in real samples.

Conclusion

This study has demonstrated that graphene oxide and layered double hydroxides composite can be easily constructed using a co-electrodeposition technique on the surface of bare GCE, and that the G-LDH composite modified GCE is fairly stable and reproducible in the electrochemical determination of HQ. Well-separated peaks and the significantly enhanced peak currents of dihydroxybenzene isomers were observed at the G-LDH/GCE, which clearly indicates that the modified electrode can be utilized for selective and sensitive detection of HQ simultaneously by using cyclic voltammetry and DPV. Under optimum conditions, the G-LDH/GCE showed well-separated oxidation peak potentials in a mixture of HQ, CA and RE. It also showed a low detection limit, good linearity and reliable recovery data in local tap water samples. These results demonstrate that the G-LDH/GCE can be used to analyze environmental samples containing HQ.

References

1. Rueda, M. E.; Sarabia, L. A.; Herrero, A.; Ortiz, M. C. *Anal. Chim. Acta* **2003**, *479*, 173.
2. Xie, T.; Liu, Q.; Shi, Y.; Liu, Q. *J. Chromatogr. A* **2006**, *1109*, 317.
3. Fujino, K.; Yoshitake, T.; Kehr, J.; Nohta, H.; Yamaguchi, M. *J. Chromatogr. A* **2003**, *1012*, 169.
4. Sirajuddin; Bhanger, M. I.; Niaz, A.; Shah, A.; Rauf, A. *Talanta* **2007**, *72*, 546.
5. Qi, H.; Zhang, C. *Electroanalysis* **2005**, *17*, 832.
6. Wang, L.; Huang, P. F.; Bai, J. Y.; Wang, H. J.; Zhang, L. Y.; Zhao, Y. Q. *Microchimica Acta* **2007**, *158*, 151.
7. Zhao, D.-M.; Zhang, X.-H.; Feng, L.-J.; Jia, L.; Wang, S.-F. *Colloids Surf., B* **2009**, *74*, 317.
8. Yin, H.; Zhang, Q.; Zhou, Y.; Ma, Q.; liu, T.; Zhu, L.; Ai, S. *Electrochim. Acta* **2011**, *56*, 2748.
9. Cavani, F.; Trifirò, F.; Vaccari, A. *Catalysis Today* **1991**, *11*, 173.
10. de Melo, J. V.; Cosnier, S.; Mousty, C.; Martelet, C.; Jaffrezic-Renault, N. *Anal. Chem.* **2002**, *74*, 4037.
11. Williams, G. R.; O'Hare, D. *J. Mater. Chem.* **2006**, *16*, 3065.
12. Touati, S.; Mansouri, H.; Bengueddach, A.; de Roy, A.; Forano, C.; Prevot, V. *Chem. Commun.* **2012**, *48*, 7197.
13. Sels, B.; Vos, D. D.; Buntinx, M.; Pierard, F.; Kirsch-De Mesmaeker, A.; Jacobs, P. *Nature* **1999**, *400*, 855.
14. Li, M.; Ni, F.; Wang, Y.; Xu, S.; Zhang, D.; Chen, S.; Wang, L. *Electroanalysis* **2009**, *21*, 1521.
15. Gong, J.; Wang, L.; Song, D.; Zhu, X.; Zhang, L. *Biosens. Bioelectron.* **2009**, *25*, 493.
16. Bai, P.; Fan, G.; Li, F. *Materials Letters* **2011**, *65*, 2330.
17. Gao, Z.; Wang, J.; Li, Z.; Yang, W.; Wang, B.; Hou, M.; He, Y.; Liu, Q.; Mann, T.; Yang, P.; Zhang, M.; Liu, L. *Chem. Mater.* **2011**, *23*, 3509.

18. Wang, L.; Wang, D.; Dong, X. Y.; Zhang, Z. J.; Pei, X. F.; Chen, X. J.; Chen, B.; Jin, J. *Chem. Commun.* **2011**, *47*, 3556.
19. Malak-Polaczyk, A.; Vix-Guterl, C.; Frackowiak, E. *Energ. Fuel.* **2010**, *24*, 3346.
20. Wang, Y.; Zhang, D.; Tang, M.; Xu, S.; Li, M. *Electrochim. Acta* **2010**, *55*, 4045.
21. Zhang, Y.; Tan, Y.-W.; Stormer, H. L.; Kim, P. *Nature* **2005**, *438*, 201.
22. Li, D.; Muller, M. B.; Gilje, S.; Kaner, R. B.; Wallace, G. G. *Nat. Nanotechnol.* **2008**, *3*, 101.
23. Wu, X.; Hu, Y.; Jin, J.; Zhou, N.; Wu, P.; Zhang, H.; Cai, C. *Anal. Chem.* **2010**, *82*, 3588.
24. Wang, D.; Choi, D.; Li, J.; Yang, Z.; Nie, Z.; Kou, R.; Hu, D.; Wang, C.; Saraf, L. V.; Zhang, J.; Aksay, I. A.; Liu, J. *ACS Nano* **2009**, *3*, 907.
25. Wang, Y.; Li, Y.; Tang, L.; Lu, J.; Li, J. *Electrochem. Commun.* **2009**, *11*, 889.
26. Shan, C.; Yang, H.; Song, J.; Han, D.; Ivaska, A.; Niu, L. *Anal. Chem.* **2009**, *81*, 2378.
27. Guo, P.; Song, H.; Chen, X. *Electrochem. Commun.* **2009**, *11*, 1320.
28. Chen, D.; Feng, H.; Li, J. *Chemical Reviews* **2012**.
29. Chen, L.; Tang, Y.; Wang, K.; Liu, C.; Luo, S. *Electrochem. Commun.* **2011**, *13*, 133.
30. Guo, H.-L.; Wang, X.-F.; Qian, Q.-Y.; Wang, F.-B.; Xia, X.-H. *ACS Nano* **2009**, *3*, 2653.
31. Kovtyukhova, N. I.; Ollivier, P. J.; Martin, B. R.; Mallouk, T. E.; Chizhik, S. A.; Buzaneva, E. V.; Gorchinskiy, A. D. *Chem. Mater.* **1999**, *11*, 771.
32. Yarger, M. S.; Steinmiller, E. M. P.; Choi, K.-S. *Inorg. Chem.* **2008**, *47*, 5859.
33. Du, H.; Ye, J.; Zhang, J.; Huang, X.; Yu, C. *J. Electroanal. Chem.* **2011**, *650*, 209.
34. Bai, J.; Guo, L.; Ndamanisha, J. C.; Qi, B. *J. Appl. Electrochem.* **2009**, *39*, 2497.
35. Li, J.; Liu, C.-Y.; Cheng, C. *Electrochim. Acta* **2011**, *56*, 2712.
36. Zhang, D.; Peng, Y.; Qi, H.; Gao, Q.; Zhang, C. *Sens. Actuators, B* **2009**, *136*, 113.
37. Ahammad, A. J. S.; Sarker, S.; Rahman, M. A.; Lee, J.-J. *Electroanalysis* **2010**, *22*, 694.
38. Ghanem, M. A. *Electrochem. Commun.* **2007**, *9*, 2501.